Environmental Science & Technology

pubs.acs.org/est

Article

Burn Intensity Drives the Alteration of Phenolic Lignin to (Poly) Aromatic Hydrocarbons as Revealed by Pyrolysis Gas Chromatography−Mass Spectrometry (Py-GC/MS)

Huan Chen, Jun-Jian Wang, Pei-Jia Ku, Martin Tsz-Ki Tsui, Rebecca B. Abney, Asmeret Asefaw Berhe, Qiang Zhang, Sarah D. Burton, Randy A. Dahlgren, and Alex T. Chow*

Cite This: https://doi.org/10.1021/acs.est.2c00426

Read Online

ACCESS | Metrics & More | Article Recommendations | Supporting Information

ABSTRACT: High-intensity wildfires alter the chemical composition of organic matter, which is expected to be distinctly different from low-intensity prescribed fires. Herein, we used pyrolysis gas chromatography/mass spectrometry (Py-GC/MS), in conjunction with solid-state ^{13}C nuclear magnetic resonance (NMR) and Fourier transform infrared (FT-IR) spectroscopy, to assess chemical alterations from three wildfires and a long-term frequent prescribed fire site. Our results showed that black ash formed under moderate intensity burns contained less aromatic (ArH), polyaromatic hydrocarbon (PAH), and nitrogen-containing compounds (Ntg) but more lignin (LgC) and phenol compounds (PhC), compared to white ash formed under high intensity burns. Both ^{13}C NMR and FT-IR confirmed a higher relative percentage of carboxyl carbon in white ash, indicating the potential for higher water solubility and more mobile carbon, relative to black ash. Compared to wildfires, ash from low-intensity prescribed fire contained less ArH, PAH, and Ntg and more LgC and PhC. Controlled laboratory burning trials indicated that organic matter alteration was sensitive to the burn temperature, but not related to the fuel type (pine vs fir) nor oxygen absence/presence at high burn temperatures. This study concludes that higher burn temperatures resulted in higher (poly)aromatic carbon/nitrogen and lower lignin/phenol compounds.

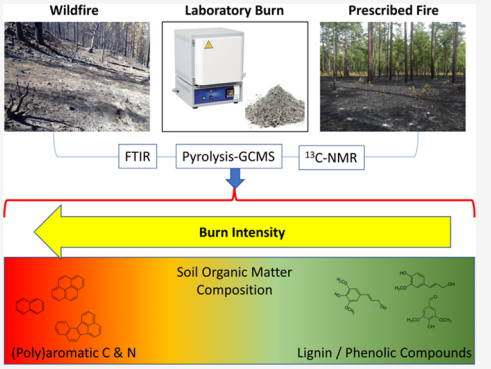

KEYWORDS: *wildfire, prescribed fire, forest fuel reduction, black carbon/nitrogen, alkyl side chain*

1. INTRODUCTION

The frequency and severity of wildfires have increased globally in the past few decades, in part due to warming trends associated with climate change.[1−3] Though poorly understood, ecosystem responses to wildfire are critical for sustained delivery of clean water[4−6] and ecosystem productivity.[7−9] These responses include changes in soil properties,[10] particularly soil organic matter (SOM), which is the most important and reactive soil fraction.[8,11] Quantitative and qualitative changes in wildfire-induced SOM are commonly ascribed to the loss of organic matter, transformation of chemical structures, and accumulation of newly-formed compounds.[11−14] The principal effect on qualitative SOM characteristics is the formation of condensed aromatic structures, including pyrogenic carbon and nitrogen, through incomplete combustion during wildfires.[15] However, because of the heterogeneity of the fuel type, oxygen availability, and burn temperature, detritus materials comprising the forest floor do not experience the same burn intensity across the landscape,[16] which affects the spatial distribution[17] and chemical composition of SOM and pyrogenic organic matter (PyOM). Further, prescribed burning/fire, as a fuel reduction technique in forest management,[18,19] is widely used for reducing the susceptibility of forests to wildfires.[19−21] Compared to wildfires, prescribed fires are low intensity,[22] which creates a sharply contrasting environment from wildfires, for the alteration of organic structures.[23,24] Therefore, investigation of how burn intensity interacts with the components of the fire triangle (including heat, oxygen, and fuel type) to affect the chemical structure of organic matter is highly warranted to enhance our understanding of the impact of changing global fire regimes on soils, forest productivity, and environmental concerns.

Pyrolysis gas chromatography/mass spectrometry (Py-GC/MS) is a frequently used technique for determining the molecular fingerprint of complex organic matrices.[11,25,26] This technique fragments large organic molecules via pyrolysis (a

Received: January 25, 2022
Revised: June 8, 2022
Accepted: July 15, 2022

thermal decomposition in the absence of oxygen).[27] Subsequently, GC separates the gaseous pyrolysates, based on their relative affinity for the column stationary phase, and MS detects the mass-to-charge ratios of the ionized fragments. The fragments are subsequently related to their parent molecules,[11,28] with the Py-GC/MS data interpretation requiring a good understanding of the pyrolysis process on the original complex molecules. Herein, we used this systematic Py-GC/MS approach, in conjunction with solid-state ^{13}C nuclear magnetic resonance (NMR) and Fourier transform infrared (FT-IR) spectroscopy, to assess burn products in ash materials from three California wildfires (2013 Rim Fire, 2015 Rocky Fire, and 2015 Wragg Fire), a long-term (since 1978) frequent prescribed fire site in South Carolina, and a laboratory burning experiment (using detritus from *Pinus ponderosa* and *Abies concolor* burned at 250, 400, and 550 °C in the presence/absence of oxygen). Our specific objectives were to (i) determine changes in the chemical composition of organic materials by high-intensity wildfires versus low-intensity prescribed fire; (ii) track the pyrogenic alteration products at the molecular scale for the long-term frequent prescribed fire site; and (iii) examine the effects of the fuel type, oxygen availability, and burn temperature on pyrogenic alteration products from a controlled laboratory burning.

2. MATERIALS AND METHODS

2.1. Sample Collection. Paired black and white ash samples were collected immediately after the 2013 Rim Fire (15 white [Rim-WA] and 15 black [Rim-BA]),[29] 2015 Rocky Fire (9 white [Rocky-WA] and 9 black [Rocky-BA]),[30] and 2015 Wragg Fire (5 white [Wragg-WA] and 5 black [Wragg-BA])[30] in northern California (see Section S1, Supporting Information). No post-fire rainfall/leaching occurred before sample collection. We used a stainless-steel hand shovel to separate and collect the surficial ash from the underlying soil. For subsequent analysis, samples were air-dried, passed through a 2 mm sieve, and stored in sealed jars in a ventilated and dry indoor environment. The prescribed fire was performed in nine management units (~1−2 ha) at the Tom Yawkey Wildfire Center in Georgetown, SC (See Section S1, Supporting Information).[24] An additional unit (~6−7 ha) that had not been burned or harvested since 1978 was used as a long-term unburned control (labeled as no-burn, 20 detritus samples comprised of litter and duff). We collected 1 × 1 m samples of litter (6 samples from the Oi horizon) and duff (6 samples from Oe + Oa horizons) before burning and the remaining ash materials after burning (23 ash samples). For subsequent analysis, samples were oven-dried at 50 °C for not less than 48 h, ground and passed through a 2-mm sieve, and stored in sealed jars in a ventilated and dry indoor environment.

A laboratory burning experiment was performed to assess the specific effects of heat, oxygen availability, and fuel type on the ash composition.[31] Briefly, non-burned detritus was collected from the surface litter, beneath ponderosa pine (*P. ponderosa*) and white fir (*A. concolor*), which are representative vegetation types outside the 2013 Rim Fire perimeter.[29] Detritus (~30 g; comprised of litter and duff) was burned at three temperatures (250, 400, and 550 °C) in a preheated muffle furnace in the presence (combustion) and absence (pyrolysis) of oxygen for 1 h.[31] All samples were weighed before and after heating, and the percentage of mass remaining was determined (Table S1). This experimental design resulted in a total of seven individual treatments: unburned (unb50); pyrolyzed at 250, 400, and 550 °C (py250, py400, and py550); and thermally oxidized at 250, 400, and 550 °C (com250, com400, and com550). Thus, we analyzed a total of 14 samples (2 fuel types × 7 burn conditions) from the laboratory burning.

2.2. Pyrolysis GC/MS. The Py-GC/MS method[32] was employed for all samples, using a pyrolysis probe (CDS 5000, CDS Analytical, Oxford, PA, USA) connected with the Agilent GC7980 gas chromatograph and 220-ion trap mass spectrometer (Agilent, Santa Clara, CA, USA) (see Section S2, Supporting Information). The automated pipeline method[33] was used for extracting pyrolysate information (S/N ≥ 3) from the raw Py-GC/MS data. Specifically, pyrolysates were automatically classified into eight chemical classes: aromatic hydrocarbons (ArH; 34 pyrolysates), polyaromatic hydrocarbons (PAH; 13 pyrolysates), nitrogen-containing compounds (Ntg; 46 pyrolysates), lignin compounds (LgC; 22 pyrolysates), phenol compounds (PhC; 21 pyrolysates), carbohydrates (Carb; 68 pyrolysates), saturated hydrocarbons (SaH; 9 pyrolysates), and unsaturated hydrocarbons (UnSaH; 28 pyrolysates) (Tables S2 and S3). In each sample, the identified pyrolysates were semi-quantified by dividing the peak area of their major fragment ions by the total peak area of all identified pyrolysates' major fragment ions.[33,34]

2.3. Solid-State ^{13}C NMR and FT-IR. To confirm and support the findings from the Py-GC/MS analysis, selected samples representative of the full dataset were characterized by solid-state ^{13}C NMR and FT-IR. Specifically, samples from wildfires (3 pairs from Rim Fire and 1 pair from Rocky and Wragg Fires) and the laboratory burning experiment (7 samples related to pine) were analyzed by solid-state ^{13}C NMR, using solid-state ^{13}C cross polarization magic angle spinning (CPMAS) NMR.[35] The solid-state ^{13}C NMR spectra were split into seven shift regions of alkyl-C (10−45 ppm), methoxy-C (45−60 ppm), *O*-alkyl-C (60−90 ppm), di-*O*-alkyl-C (95−110 ppm), aromatic-C (110−145 ppm), *O*-aromatic-C (145−165 ppm), and carboxyl-C (160−210 ppm). Samples from the Rim Fire (15 pairs) and the laboratory burning experiment (14 samples) were characterized by diffuse reflectance infrared Fourier-transform infrared spectroscopy (FT-IR) under vacuum on the Bruker IFS 66v/S FT-IR (Billerica, MA)[36] at the University of California-Merced. FT-IR spectra were obtained by integrating 64 scans over a 4000−400 cm^{-1} background corrected using a KBr spectrum and baseline corrected using OPUS software (version 6.5). Spectral peaks were assigned to O−H stretching (hydroxyl-C) at 3700 and 3625 cm^{-1}, aliphatic C−H stretching at 2940 and 2850 cm^{-1}, O−H stretching (carboxyl-C) at 2500 and 1430 cm^{-1}, C≡N stretching at 2222 cm^{-1}, C═O stretching at 1795 cm^{-1}, and C═C bending (aromatic-C) at 1600, 875, and 790 cm^{-1} (www.sigmaaldrich.com/technical-documents/articles/biology/ir-spectrum-table.html).[14,36]

2.4. Data Analysis. We used RStudio Desktop version 1.2.1335 (Boston, MA, USA) for statistical analysis and data visualization. One-way analysis of variance (ANOVA) and post-hoc Tukey HSD were conducted using the *aov* and *HSD.test* function in the *stats* and *agricolae* package, respectively. Hierarchical clustering, measuring the dissimilarity of pyrolysates by their relative area percentages, was conducted with the *hclust* function in the *stats* package and visualized by the *circlize_dendrogram* function in the

https://doi.org/10.1021/acs.est.2c00426
Environ. Sci. Technol. XXXX, XXX, XXX−XXX

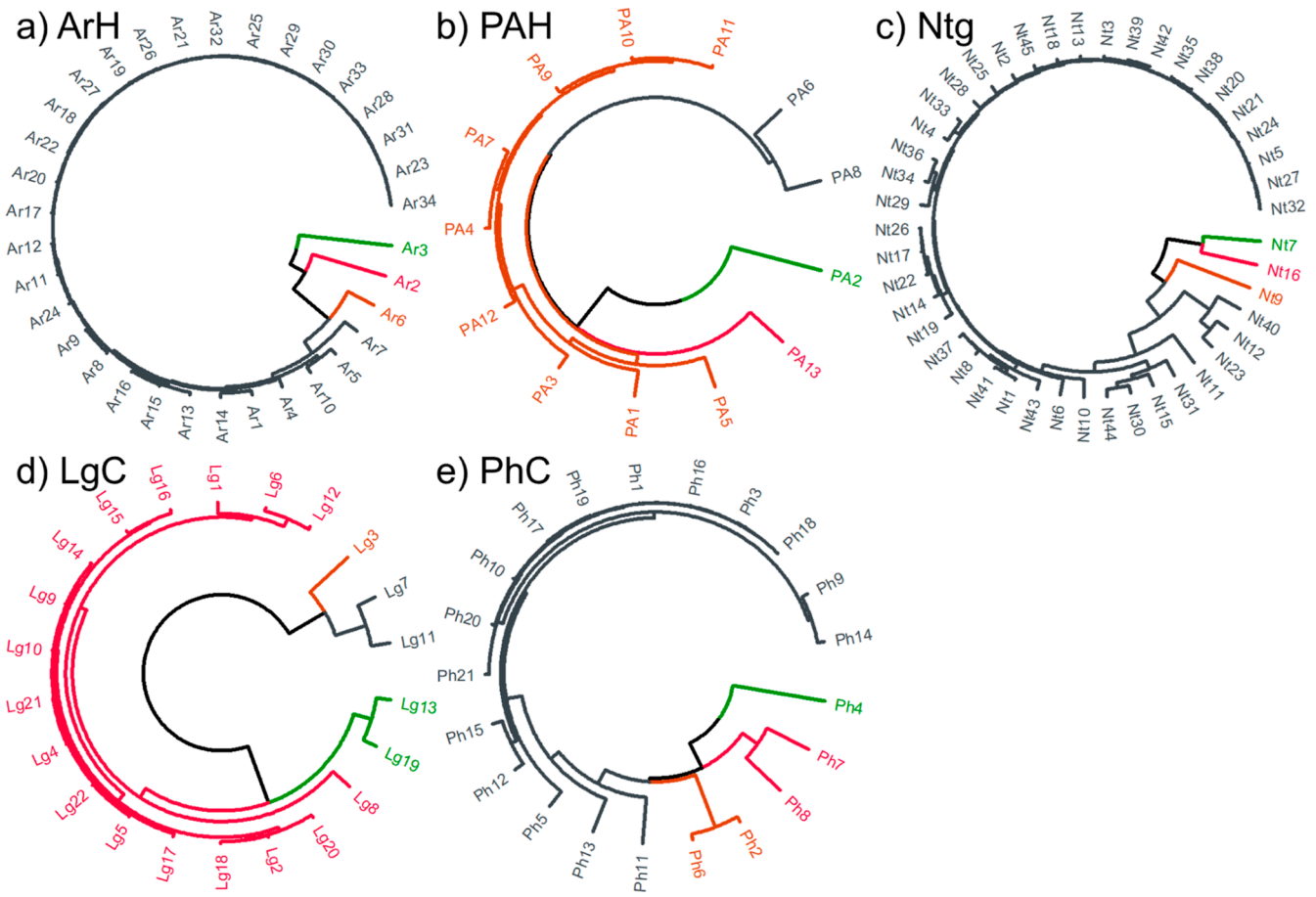

Figure 1. Hierarchical clustering based on the relative area percentages of identified pyrolysis products in all samples. Color code: green = cluster 1, red = cluster 2, brown = cluster 3, and black = cluster 4. Additional information about identified pyrolysis products is presented in Table S2. ArH: aromatic hydrocarbons; PAH: polyaromatic hydrocarbons; Ntg: nitrogen-containing compounds; LgC: lignin compounds; PhC: phenol compounds.

dendextend package.[37] Factor analysis used the *fa* functions in the *psych* package for highlighting differences in pyrolysates among samples.

3. RESULTS

3.1. Pyrolysate Chemical Classes. Ash samples from wildfires contained higher ArH, PAH, and Ntg and lower LgC and PhC, compared to ash samples from the prescribed fire (Table S3). Wildfire black ash contained less ArH, PAH, and Ntg and more LgC, PhC, Carb, SaH, and UnSaH, compared to white ash. For example, the black versus white ash from the three wildfires had average percentages of 29.7−43.6% versus 45.2−79.1% for ArH, 2.3−2.8% versus 4.6−5.6% for PAH, 8.3−13.0% versus 9.1−25.3% for Ntg, 3.9−6.5% versus < 0.1−0.2% for LgC, and 17.2−24.1% versus 0.1−8.8% for PhC. For the prescribed fire, LgC and PhC were the dominant chemical classes in all sample types (noburn, litter, duff, and ash), accounting for 28.7−40.2 and 33.0−43.2%, respectively. ArH comprised low percentages (mean ± standard deviation) of 5.4 ± 2.1, 6.1 ± 1.7, 8.0 ± 1.9, and 7.9 ± 1.6% in the no-burn, litter, duff, and ash samples. Moreover, PAH was only detected in ash samples but at very low percentages (0.5 ± 0.5%).

For the controlled laboratory burning samples, both ArH and PAH progressively increased with increasing temperature (50−550 °C) under pyrolysis conditions (O_2 absent). Specifically, as the temperature increased (unb50, py250, py400, and py550) percentages of ArH were 22.3 ± 1.6, 25.9 ± 3.9, 36.6 ± 6.0, and 52.0 ± 5.1%, and percentages of PAH were 0.4 ± 0.5, 0.5 ± 0.7, 4.9 ± 1.3, and 16.1 ± 18.9%. The LgC component completely disappeared at temperatures of 400 and 550 °C, while PhC was not found at 550 °C. Under combustion conditions (O_2 present), ArH progressively increased with increasing temperature. In contrast, PAH increased as the temperature increased from 50 to 250 °C, but then decreased as the temperature further increased to 550 °C. Specifically, for com250, com400, and com550 samples, percentages of ArH were 45.0 ± 3.4, 47.6 ± 9.5, and 50.8 ± 3.7%, and percentages of PAH were 3.4 ± 0.4, 2.5 ± 1.7, and 1.5 ± 0.4%, respectively. The LgC component completely disappeared at 250, 400, and 550 °C, while PhC was not found at 400 and 550 °C. Notably, at 250, 400, and 550 °C, the average Ntg percentage was in the range of 24.0−41.1%, which was much higher than 4.9−6.0% under pyrolysis conditions. This result indicates that combustion conditions favored Ntg accumulation, relative to pyrolysis conditions. Notably, the remaining percentage of the original detritus mass decreased with increasing temperature, with a more pronounced decrease for combustion versus pyrolysis conditions (Table S1).

3.2. Pyrolysate Chemical Clusters. The occurrence and relative peak-area percentage of pyrolysates, considered fingerprints of the complex organic matrix (Figure S2), were highly variable among samples, creating challenges for

https://doi.org/10.1021/acs.est.2c00426
Environ. Sci. Technol. XXXX, XXX, XXX−XXX

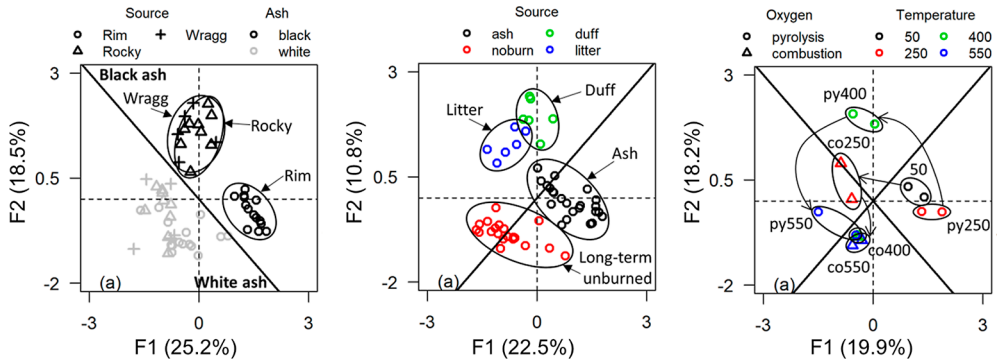

Figure 2. Scores of each sample in F1 and F2 during factor analysis of the pyrolysates in samples from (a) three wildfires; (b) long-term frequent prescribed fire; and (c) laboratory experiment.

interpretation.[33] Using hierarchical clustering, the pyrolysates in each chemical class were grouped into four clusters (Figure 1), and the pyrolysates inside each cluster had similarities in the relative area percentages. The ArH class contained benzene (Ar2; cluster 2), toluene (Ar3; cluster 1; benzene with a C_1 alkyl side chain), and *p*-xylene (Ar6; cluster 3; benzene with two C_1 alkyl side chains). The PAH class included naphthalene (PA2; cluster 1), 1-methyl-7-(1-methylethyl)-phenanthrene (PA13; cluster2; phenanthrene with a C_1 and C_3 alkyl side chain), 1,3-dimethyl-naphthalene (PA6; cluster 4; naphthalene with two C_1 alkyl side chains), and 1,6,7-trimethyl-naphthalene (PA8; cluster 4; naphthalene with three C_1 alkyl side chains). The Ntg class contained pyridine (Nt7; cluster 1), benzonitrile (Nt16; cluster 2), and 2-methyl-1h-pyrrole (Nt9; cluster 3; pyrrole with a C_1 alkyl side chain).

Benzene (Ar2), toluene (Ar3), and naphthalene (PA2) are considered characteristic constituents of BC,[38] while benzonitrile (Nt16) belongs to black nitrogen (BN). Samples from wildfires, prescribed fire, and laboratory burning (total samples = 127; n_{det} = samples with detectable concentrations) had Ar2 percentages of 2.11−72.5% (n_{det} = 57), 0.3−1.6% (n_{det} = 44), and 1.0−50.1% (n_{det} = 14); Ar3 percentages of 3.2−45.4% (n_{det} = 58), 1.8−6.0% (n_{det} = 55), and 5.1−20.6% (n_{det} = 13); and PA2 percentages of 0.5−5.2% (n_{det} = 58), 0.4% (n_{det} = 1) and 0.7−25.5% (n_{det} = 10), respectively (Table S2). White ash had much higher Ar2 and PA2 percentages than black ash in wildfire events (Table S4). At each laboratory burning temperature, combustion produced higher Ar2 percentages than pyrolysis. Average PA2 percentages at 250, 400, and 550 °C were 1.5, 1.9, and 1.3% by combustion and <0.01, 0.7, and 13.8% by pyrolysis. Wildfire events produced higher PA2 percentages in white versus black ash, and no PA2 was identified in unb50 and prescribed fire-derived samples (noburn, litter, duff, and ash). Combustion samples had the highest average N16 percentages of 20.5, 30.9, and 23.4% at 250, 400, and 550 °C, respectively. Nt7, Nt9, and Nt16 were not identified in samples from the prescribed fire study, except for 0.1 ± 0.3% of Nt7 in duff.

The LgC class contained 4-ethyl-2-methoxy-phenol (Lg13; cluster 1), 2-methoxy-4-(1-propenyl)-phenol (Lg19; cluster 1), 2-methoxy-phenol (Lg3; cluster 3), 2-methoxy-4-methylphenol (Lg7; cluster 4), and 2-methoxy-4-vinylphenol (Lg11; cluster 4). Lg11 is considered as a pyrolytic marker for guaiacol (G) lignin.[39,40] Laboratory burning identified Lg3, Lg7, Lg11, Lg13, and Lg19 only in unb50 and py250 treatments. Moreover, these five compounds were not identified in white ash samples, except for Lg3 in Rim-WA. Pyrolysates in the PhC class included (Ph4; cluster 1), 2-methylphenol (Ph7; cluster 2; phenol with a C_1 alkyl side chain), 4-methylphenol (Ph8; cluster 2; phenol with a C_1 alkyl side chain), 1,2-benzenediol (Ph2; cluster 3), and 4-methyl-1,2-benzenediol (Ph6; cluster 3; 1,2-benzenediol with a C_1 alkyl side chain). The pyrolysates of Lg3, Lg7, Lg13, and Lg19 are methoxyphenols originating from the degraded lignin,[41] while Ph7-8 are methylphenols from demethylated or/and demethoxylated lignin.[34,42] Ph2 and Ph6 were only identified in unb50 and prescribed fire-derived samples (noburn, litter, duff, and ash). Ph4 and Ph7-8 were not found in py550, com250, com400, and com550 samples, except for Ph7-8 in the com250 sample. These three compounds (Ph4, Ph7, and Ph8) had higher average percentages in black ash versus white ash for wildfire events.

3.3. Factor Analysis. Factor analysis identified two factors (F1 and F2) to assist in interpreting pyrolysate differences among samples. For wildfires, the two factors explained 25.2 and 18.5% of the total variance (Figure 2a), with the interpretation of LgC, PhC, and Carb, associated with the positive F1 and Carb related to the positive F2. Specifically, F1 was positively (F1 loading ≥ 0.50) correlated with 4 of the 6 identified LgC (denoted as 4/6), PhC (5/6), and Carb (8/20), while pyrolysates with F2 loading ≥0.50 included Carb (7/20) (Table S5). The diagonal line of F2 = −F1 provided good separation for points in the F1 − F2 loading and score projections. Most of the identified ArH (13/15), PAH (4/9), Ntg (14/19), LgC (6/6), PhC (6/6), Carb (15/20), SaH (4/4), and UnSaH (8/8) were located on the top-right side of this line. In contrast, PAH (5/9) (including naphthalene [PA2], 1,2-dihydro-naphthalene [PA3], biphenyl [PA5], fluorene [PA7] and phenanthrene [PA9]), and ArH (2/15) (including benzene [Ar2] and styrene [Ar7]) were positioned on the bottom-left side of this diagonal line. Notably, the F1 − F2 score projection effectively separated the white (top-right) and black (bottom-left) ash samples by the diagonal line of F1 + F2 = 0.

For prescribed fires, F1 and F2 accounted for 22.5 and 10.8% of the total variance (Figure 2b). Specifically, the positive F1 (F1 loading ≥ 0.50) was correlated with ArH (5/10), PAH (1/4), PhC (6/17), and SaH (2/3), while the negative F1 (F1 loading ≤ −0.50) was related to Ntg (4/15) and LgC (6/21). The diagonal F2 = F1 line in the F1 − F2 projection provided a good separation for both sample scores and pyrolysate loading. Specifically, the cluster of litter and duff samples were above the diagonal line, which crossed the cluster of no-burn samples (10 samples on each side). Additionally, the cluster of ash samples (except 4 of 23 samples) was on the

https://doi.org/10.1021/acs.est.2c00426
Environ. Sci. Technol. XXXX, XXX, XXX−XXX

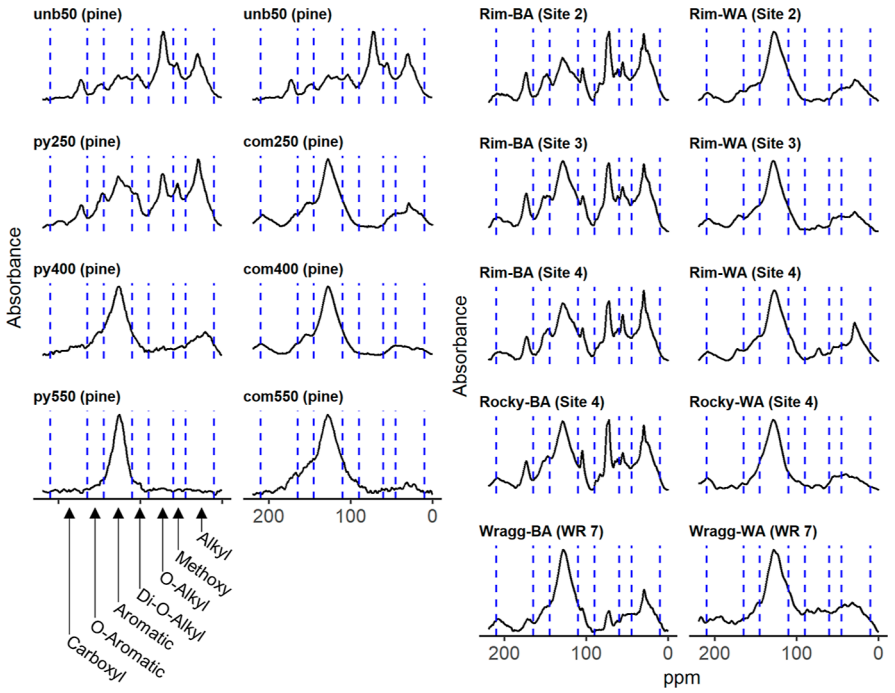

Figure 3. Solid-state ^{13}C NMR spectra for selected samples from wildfires and the laboratory burning experiment. Spectra were characterized into seven shift regions of alkyl-C (10−45 ppm), methoxy-C (45−60 ppm), O-alkyl-C (60−90 ppm), di-*O*-alkyl-C (95−110 ppm), aromatic-C (110−145 ppm), O-aromatic-C (145−165 ppm), and carboxyl-C (160−210 ppm). Information about the sampling sites for each paired ash sample is presented by Wang et al.[29] for the Rim Fire and in Ku et al.[30] for the Rocky and Wragg Fires.

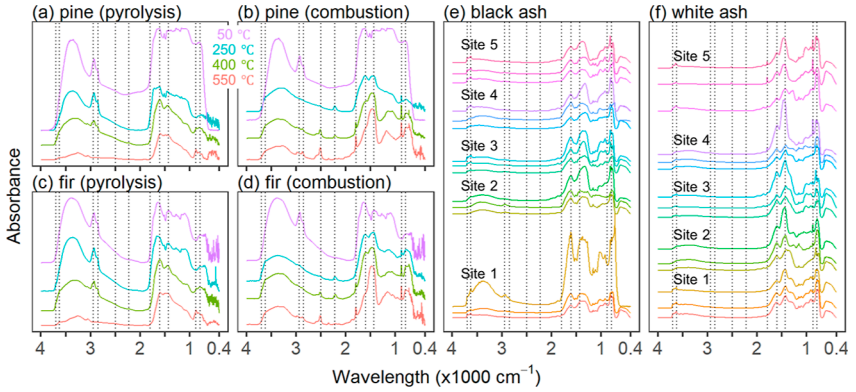

Figure 4. FT-IR spectrum on selected samples from wildfires and laboratory burn experiment. From left to right, the wavelength of dotted black lines was 3700, 3625, 2940, 2850, 2500, 2222, 1795, 1600, 1430, 875, and 790 cm^{-1}. Spectral peaks were assigned to O−H stretching (hydroxyl-C) at 3700 and 3625 cm^{-1}, aliphatic C−H stretching at 2940 and 2850 cm^{-1}, O−H stretching (carboxyl-C) at 2500 and 1430 cm^{-1}, C≡N stretching at 2222 cm^{-1}, C═O stretching at 1795 cm^{-1}, and C═C bending (aromatic-C) at 1600, 875, and 790 cm^{-1}. Information about the sampling sites of each paired ash sample is presented by Wang et al.[29]

bottom-right side of the line. Most of the identified Ntg (11/15) and LgC (19/21) components were above the diagonal line, whereas most of the identified ArH [9/10; except styrene (Ar7)], PAH (4/4), PhC (13/17), SaH (3/3), and UnSaH (9/13) were below the diagonal line.

For laboratory burning samples, F1 (19.9% of total variance) was positively correlated (F1 loading ≥ 0.50) with LgC (7/9) and Carb (14/32), while F2 (18.2% of the total variance) was positively related (F2 loading ≥ 0.50) with ArH (10/25), PAH (6/11), and PhC (8/13) (Figure 2c). Notably, the diagonal (F2 = F1) line effectively separated ArH (20/25), PAH (9/11), SaH (6/6), and UnSaH (13/17) in the top-left quadrant, whereas most of the identified PAH (8/11), Ntg (17/23), LgC (9/9), PhC (13/13), Carb (26/32), and SaH (4/6) points fell within the top-right quadrant separated by the F2 = −F1 diagonal line.

4. DISCUSSION

4.1. High-Intensity Wildfires. Black ash contained relatively higher percentages of lignin-derived compounds than the white ash, though pyrogenic aromatic carbon and nitrogen were found in black ash. The F1 − F2 score projection separated the black and white ash (Figure 2a), suggesting that these two ash types contained different abundances of pyrolysates across all wildfire sources. Incomplete combustion leads to the production of pyrogenic aromatic compounds through a decrease of *O*-alkyl and an increase of aromatic and *O*-aromatic structures,[43] as supported

https://doi.org/10.1021/acs.est.2c00426
Environ. Sci. Technol. XXXX, XXX, XXX−XXX

by enrichment of ArH, such as ethylbenzene (Ar5) and p-xylene (Ar6) in black ash. Using solid-state ^{13}C NMR, we observed a higher peak area of *O*-alkyl-C (60−90 ppm; mainly associated with sugars and polysaccharides[44]) in black ash from the Rim and Rocky wildfires compared to their corresponding white ash. Higher relative percentages of both aromatic-C (110−145 ppm) and *O*-aromatic-C (145−165 ppm) were also observed in white ash from the Rim and Rocky wildfires, compared to the black ash (Figure 3 and Table S6). Pyrogenic aromatic nitrogen was generated during charring, as evidenced by the pyrolysates of benzyl nitrile (Nt19) that were relatively abundant in black ash. Notably, solid-state ^{13}C NMR identified a higher relative percentage of carboxyl-C (160−210 ppm) in white ash, compared to black ash, suggesting a potential for higher water solubility and more mobile C in white ash.[45] This was confirmed by the higher 1430 cm^{-1} peak (carboxyl group) in the FT-IR spectra of white ash, relative to black ash (Figure 4).

Previous studies did not identify lignin at charring temperatures ≥400 °C.[42,46] Kaal et al.[46] reported that products with 4-hydroxy-3-methoxyphenyl or 3,5-dimethoxy-4-hydroxyphenyl moieties, signifying lignin markers, decreased with increasing charring temperature up to 400 °C due to the demethoxylation and demethylation of methoxylic groups in lignin. The LgC and PhC classes, mainly originating from lignin via depolymerization and demethoxylation,[34,47,48] were considerably higher in black ash (3.9−6.5 and 17.2−24.1%) compared to their concentrations in white ash (<0.1−0.2 and 0.1−8.8%), respectively. Factor analysis also suggested a relative enrichment of LgC and PhC in black ash compared to white ash. Solid-state ^{13}C NMR spectra identified higher peaks for alkyl-C (10−45 ppm; characteristic of lipid waxes and cutins[44]) and methoxy-C (45−60 ppm; associated with lignin[44]) in black ash compared to those in white ash (Figure 3 and Table S6).

Notably, black ash from the Rim Fire was distributed at the top corner of the F1 − F2 score projection, while black ash from the Rocky and Wragg Fires displayed considerable overlap in the bottom region. When assessing samples moving from top-to-bottom along the diagonal line (F2 = −F1), an increase in lignin compounds and a decrease in aromatic compounds were observed (Table S3), possibly attributable to decreasing burn temperature. This evidence suggests that black ash from the Rim Fire experienced relatively lower burn temperatures than black ash from the Rocky and Wragg Fires. In fact, solid-state ^{13}C NMR analysis showed relatively lower percentages of both *O*-alkyl-C and di-*O*-alkyl-C in black ash from the Rocky and Wragg Fires, compared with those from the Rim Fire (Figure 3 and Table S6). These results are consistent with the much higher fuel load contained in the dense coniferous forest comprising the Rim Fire, as compared to a lower fuel load associated with the predominant shrublands within the Rocky and Wragg Fires.

White ash displayed a relative dominance of pyrolysates derived from BC and BN, when compared to black ash. The location of white ash samples on the bottom-left side in the F1 − F2 score projection indicates enrichment of Ar2, Ar7, PA2, PA3, PA5, PA7, PA9, Nt7, Nt13, Nt16-17, Nt24, Ca3, Ca27, Ca33, Ca38, and Ca50. Most of these pyrolysates are considered indicative of BC and BN compounds.[38,49] For example, Kaal et al.[38] considered aromatic compounds including benzene (Ar2), toluene (Ar3), PAHs [naphthalene (PA2), biphenyl (PA5), fluorene (PA7), and phenanthrene (PA9)], and N- and O-containing (poly) aromatics [dibenzofuran (Ca50) and benzonitrile (Nt16)] as characteristic compounds comprising BC. González-Pérez et al.[27] proposed PAHs with three (PA9) and four benzene rings as the indicators of charred or burnt materials. Moreover, most of these enriched pyrolysates are aromatic compounds without alkyl side chains. Kaal and Rumpel[50] reported an increase in benzene/toluene and naphthalene/C_1-naphthalene with increasing pyrolysis temperature. They posited that increased charring temperature resulted in the loss of alkyl side chains from aromatic pyrolysis products due to side-chain burn-off or aromatization, which would coincide with polycondensation to fused aromatics.

Alexis et al.[51] summarized the structural changes of natural organic matter with the heating temperature of fires. Briefly, dehydration and aromatic core formation occurred at temperatures >150 °C, which induces fewer *O*-alkyl and more aromatic structures. Enrichment of aromatic compounds was further enhanced by *O*-alkyl degradation at temperatures >250 °C, and polyaromatic compounds were formed at >350 °C. Therefore, we ascribe the factor analysis results to indicate that white ash from wildfires had higher aromaticity and aromatic condensation than black ash. This inference is supported by the relatively higher average percentages of ArH, PAH, and Ntg in white ash, compared to black ash, in each of the three wildfire events and confirmed by the results from solid-state ^{13}C NMR.

4.2. Low-Intensity Prescribed Fire. Prescribed fire samples were separated into four clusters in the F1 − F2 score projection, corresponding to the four contrasting sample types (Figure 2b). The F1 − F2 score projection for litter and duff samples was above the F1 = F2 diagonal line, suggesting a relative enrichment of LgC and Ntg compounds. The LgC class originates from lignin and exclusively has a plant material source,[34] while Ntg originates from proteins that may have either a microbial or plant material source.[34,52] Among the pyrolysates located in this region, indoles [1,3-dimethyl-1*H*-indole (Nt28)] are reported to be associated with the plant material.[28,34] We posit that prescribed fire for fuel removal enhances vegetation richness[53] and plant productivity,[13] possibly due to the accumulation of soil available nutrients by pyromineralization from the forest litter.[22,53] Our study indicates that the effects of long-term frequent prescribed fire on the chemical composition of organic compounds was successfully tracked by factor analysis, based on the percentage of pyrolysates from Py-GC/MS. Prescribed fire effects on the soil quality were previously reported to be negligible or minor at larger scales[13,24,53] due to relatively lower burn temperatures of 490 ± 110 °C.[51] For example, Ranatunga et al.[23] concluded that low-intensity prescribed fire caused limited structural changes (e.g., dehydrogenation, deoxygenation, and decarboxylation) in SOM. Our previous study also concluded that unburned and burned detritus from the prescribed fire had a nearly uniform chemical composition, based on the percentages of chemical classes identified by pyrolysis GC/MS.[24]

Ash samples located below the diagonal line, with relatively high F1 scores (Figure 2b), indicate a relative enrichment of ArH, PAH, PhC, and SaH. ArH and PAH may derive from various origins, including lignin, polysaccharides, and proteins,[34] leading to little diagnostic value for litter decomposition. However, these organic compounds can transform into aromatic structures via incomplete combustion,[28] contributing to the relatively high abundance of aromatic

https://doi.org/10.1021/acs.est.2c00426
Environ. Sci. Technol. XXXX, XXX, XXX−XXX

structures in pyrolysates.[54] The PhC class includes phenol (Ph4) and methylphenols [including 2-methyl-phenol (Ph7) and 4-methyl-phenol (Ph8)] that may originate from microbial demethylation or thermal degradation of lignin.[28] The Carb class is generally from the plant- and/or microbial-derived polysaccharides.[55] For example, compounds based on furan moieties [including 2,5-dimethyl-furan (Ca16) and 2,3-dihydro-benzofuran (Ca28)] and cyclopentenone and cyclopentenedione structures [including 2-cyclopenten-1-one (Ca2) and 1,3-cyclopentanedione (Ca7)] originate from polysaccharides.[56] The ubiquitous presence of Carb pyrolysates in the burned (ash) and unburned (noburn, litter, and duff) samples implies that prescribed fire with comparatively low burn temperatures does not provide enough energy for deoxygenation and decarboxylation of polysaccharides. De la Rosa et al.[28] ascribed low wildfire intensities as a possible reason for the large amounts of aliphatic compounds (both alkyl- and carbohydrate-derived compounds) in ash materials.

4.3. Fire Triangle: Oxygen-Temperature-Fuel Type. The laboratory burning experiments were designed to assess the role of temperature, oxygen availability, and fuel source on organic matter transformations. While pyrolysis at 250 °C did not provide enough energy for breaking down large organic molecules in the detritus, an increase in the pyrolysis temperature from 250 to 400 °C resulted in a decrease in LgC and Carb and an increase of ArH, PAH, and PhC. The non-burned samples (50 °C) were located on the right of the F1 − F2 projection (Figure 2c), indicating a relative enrichment of Carb and LgC. Among the Carb and LgC pyrolysates with F1 loading ≥0.50, 2-methoxy-4-vinylphenol (Lg11) was derived from guaiacyl lignin, while 2,3-dihydro-benzofuran (Ca28) is a heterocyclic compound formed by recombination of allyl radical intermediate compounds during lignin pyrolysis.[57] Using solid-state ^{13}C NMR, we found large peaks assigned to alkyl-C, methoxy-C, and *O*-alkyl-C in non-burned pine detritus (Figure 3 and Table S6). Samples experiencing 250 °C pyrolysis were in close proximity to non-burned samples, suggesting that 250 °C pyrolysis was not sufficient for breaking down large molecules in the detritus. This result was further confirmed by large peaks for alkyl-C, methoxy-C, and *O*-alkyl-C in pine detritus after 250 °C pyrolysis, potentially explaining the limited structural changes of the low-intensity prescribed fire on the organic matter.

After increasing the pyrolysis temperature from 250 to 400 °C, sample scores decreased in F1 and increased in F2, suggesting a decrease of LgC and Carb and an increase of ArH, PAH, and PhC. Budai et al.[58] indicated that the thermal decomposition of *Miscanthus* lignin occurred at pyrolysis temperatures of 300−350 °C. The appearance of aliphatic hydrocarbons may be due to decarbonylation and decarboxylation reactions at ∼370 °C.[58] Knicker[13] reported a distinct change in pyrolysates from carbohydrates to phenols, furans, and aromatic hydrocarbons when temperature increased from 250 to 310 °C. The formation of PhC possibly resulted from reduction of alkoxy or *O*-alkyl to alkyl groups and upon further heating induced conversion of hydroaromatic to aromatic structures by dehydrogenation reactions.[58] FT-IR data showed a reduction in aliphatic C−H stretching peaks at 2940 and 2850 cm^{-1}, with increasing pyrolysis temperature and their complete disappearance after pyrolysis at 550 °C or combustion at 250, 400, and 550 °C (Figure 4). Moreover, we observed a higher 1430 cm^{-1} peak (carboxyl group) in samples after combustion, consistent with the relatively higher percentages of carboxyl-C (160−210 ppm), identified by solid-state ^{13}C NMR, relative to pyrolysis.

Samples experiencing pyrolysis at 550 °C or combustion at 400 and 500 °C were similarly dominated by BC- and BN-derived pyrolysates. These three clusters overlapped in the F1 − F2 score projection, although the samples after pyrolysis and combustion treatments showed different trajectories as temperature increased from 50 to 550 °C (Figure 2c). Alexis et al.[51] reported that the thermal transformation of organic compounds into aromatic structures depended on both temperature and oxygen availability, which potentially explains the different trajectories observed in our study. Pyrolysates of ArH (9/25) including benzene (Ar2), Ntg (4/23) including pyridine (Nt7) and benzonitrile (Nt16), and PAH (3/11) including naphthalene (PA2), biphenyl (PA5), and phenanthrene (PA9) were located in the third quadrant, indicating enrichment of (condensate) aromatic compounds with few alkyl side chains after pyrolysis at 550 °C or combustion at 400 and 550 °C. In contrast, the 250 °C combustion samples had smaller scores in both F1 and F2, compared to the 400 °C pyrolysis, which we ascribe to further thermal decomposition of lignin and conversion of aromatic to polyaromatic structures by the 250 °C combustion. This result potentially explained that the order of white ash in wildfires > black ash in wildfires > ash in prescribed fires in ArH and PAH.

The pyrolysates located in the third quadrant were previously observed after thermal treatments at high temperatures and attributed to BC and BN compounds.[38,49] Kaal and Rumpel[50] reported an increase of benzene (Ar2), toluene (Ar3), naphthalene [including naphthalene (PA2)], alkylnaphthalenes, benzofuran (Ca33), and benzonitrile (Nt16) and a decrease of levoglucosan (originating from polysaccharides), 4-vinylsyringol (originating from lignin), and diketodipyrrole (originating from protein and/or chlorophyll) as the pyrolysis temperature increased from 400 to 1200 °C. Xu et al.[59] reported that above 500 °C, N-heterocycle compounds were formed, but they were subsequently decomposed along with nitrile at temperatures above 600 °C. Kaal et al.[60] considered that benzonitrile (Nt16) was derived from the thermal decomposition of aromatic amines because it was plotted close to benzenes and was separated from other Ntg in the F1 − F2 projection. The previous studies[42,50] concluded a general trend of Ntg from pyrroles to pyridines and to benzonitriles with increasing char temperature. Our laboratory burning trials investigating fire triangle interactions (including the fuel type, oxygen, and temperature) suggest that thermal alterations of pine and fir detritus were affected by both oxygen and burn temperature, but the alteration products were not strongly related to the absence or presence of oxygen at high burn temperatures (>400 °C). Notably, the detritus (fuels) from pine versus fir sources did not significantly affect the pyrolysis products of any temperature/oxygen treatments, potentially because both are conifers with similar chemical compositions.

5. ENVIRONMENTAL IMPLICATIONS

We used the analytic technique of Py-GC/MS to track the chemical composition of samples from three wildfires (black and white ash samples), prescribed fire (no-burn, litter, duff, and ash samples), and a laboratory burning experiment (examining the fire triangle of the fuel type, oxygen, and temperature). Compared to black ash from the incomplete combustion or charring, white ash from the more complete combustion contained more ArH, PAH, and Ntg and less LgC

https://doi.org/10.1021/acs.est.2c00426
Environ. Sci. Technol. XXXX, XXX, XXX−XXX

and PhC. Moreover, the ash samples from the low-intensity prescribed fire had much lower ArH, PAH, and Ntg, but higher LgC and PhC than black or white ash from the high-intensity wildfires. Our study indicates that burn intensity promotes the conversion of plant-derived lignin compounds to aromatic compounds, resulting in higher (poly) aromatic carbon/nitrogen and lower lignin/phenol compounds. This result suggests that after fires with higher burn intensity, the post-fire SOM contains higher (poly) aromatic carbon/nitrogen and is potentially more resistant to biological decomposition. Therefore, we should consider burn intensity when evaluating the post-fire ecosystem recovery and estimating soil C dynamics in global ecosystem models.

The laboratory burning experiment indicated that thermal alterations of pine and fir detritus were affected by both oxygen and burn temperature, but the altered chemical compositions were not related to the absence or presence of oxygen at high burn temperatures (>400 °C). This result indicates a less important role of oxygen than burn temperatures on the organic matter composition during fires with high burn intensity. The fuel type (pine vs fir detritus) showed no detectable effects on the alteration products resulting from pyrolysis or combustion, potentially due to their similar initial chemical compositions. More research is needed to evaluate the influence of different fuel types.

■ ASSOCIATED CONTENT

Supporting Information

The Supporting Information is available free of charge at https://pubs.acs.org/doi/10.1021/acs.est.2c00426.

Sample collection, pyrolysis GC/MS, and solid-state ^{13}C NMR and FT-IR characterization; laboratory burning percentage of residual mass; the identified/quantified pyrolysates with their percentage summary and factor analysis loadings; relative area percentages of chemical classes; relative area percentages of selected pyrolysates; list of pyrolysates with high loadings; and percentages of classes by solid-state ^{13}C NMR; pyrograms for each sample type, a heat map for the average percentage of pyrolysates, and factor analysis of the pyrolysates in samples from three wildfires, the long-term frequent prescribed fire, and laboratory experiment (PDF)

■ AUTHOR INFORMATION

Corresponding Author

Alex T. Chow − *Biogeochemistry & Environmental Quality Research Group, Clemson University, Georgetown, South Carolina 29442, United States;* orcid.org/0000-0001-7441-8934; Phone: +1 843 546 1013 x232; Email: achow@clemson.edu; Fax: +1 843 546 6296

Authors

Huan Chen − *Biogeochemistry & Environmental Quality Research Group, Clemson University, Georgetown, South Carolina 29442, United States;* orcid.org/0000-0001-9998-1205

Jun-Jian Wang − *Guangdong Provincial Key Laboratory of Soil and Groundwater Pollution Control, School of Environmental Science and Engineering, Southern University of Science and Technology, Shenzhen 518055, China; State Environmental Protection Key Laboratory of Integrated Surface Water-Groundwater Pollution Control, School of Environmental Science and Engineering, Southern University of Science and Technology, Shenzhen 518055, China;* orcid.org/0000-0002-3040-0924

Pei-Jia Ku − *Environmental Sciences Division, Oak Ridge National Laboratory, Oak Ridge, Tennessee 37831, United States;* orcid.org/0000-0003-2813-9269

Martin Tsz-Ki Tsui − *School of Life Sciences, State Key Laboratory of Agrobiotechnology, The Chinese University of Hong Kong, Hong Kong SAR, China;* orcid.org/0000-0003-2002-1530

Rebecca B. Abney − *D.B. Warnell School of Forestry and Natural Resources, University of Georgia, Athens, Georgia 30602, United States*

Asmeret Asefaw Berhe − *Department of Life and Environmental Sciences, University of California, Merced, California 95343, United States*

Qiang Zhang − *Guangdong Provincial Key Laboratory of Soil and Groundwater Pollution Control, School of Environmental Science and Engineering, Southern University of Science and Technology, Shenzhen 518055, China; State Environmental Protection Key Laboratory of Integrated Surface Water-Groundwater Pollution Control, School of Environmental Science and Engineering, Southern University of Science and Technology, Shenzhen 518055, China*

Sarah D. Burton − *Environmental Molecular Sciences Laboratory, Pacific Northwest National Laboratory, Richland, Washington 99354, United States;* orcid.org/0000-0003-3077-6304

Randy A. Dahlgren − *Department of Land, Air, and Water Resources, University of California, Davis, California 95616, United States*

Complete contact information is available at: https://pubs.acs.org/10.1021/acs.est.2c00426

Notes

The authors declare no competing financial interest.

■ ACKNOWLEDGMENTS

The authors acknowledge the funding support from USEPA (National Priorities: Water Scarcity & Drought with grant number R835864), USDA NIFA (Grant Number: 2018-67019-27795), NSF (1917156), and National Natural Science Foundation of China (42192513).

■ REFERENCES

(1) Miller, J. D.; Safford, H. D.; Crimmins, M.; Thode, A. E. Quantitative evidence for increasing forest fire severity in the Sierra Nevada and Southern Cascade Mountains, California and Nevada, USA. *Ecosystems* **2009**, *12*, 16−32.

(2) Westerling, A. L.; Hidalgo, H. G.; Cayan, D. R.; Swetnam, T. W. Warming and earlier spring increase western US forest wildfire activity. *Science* **2006**, *313*, 940−943.

(3) Schoennagel, T.; Balch, J. K.; Brenkert-Smith, H.; Dennison, P. E.; Harvey, B. J.; Krawchuk, M. A.; Mietkiewicz, N.; Morgan, P.; Moritz, M. A.; Rasker, R.; Turner, M. G.; Whitlock, C. Adapt to more wildfire in western North American forests as climate changes. *Proc. Natl. Acad. Sci. U.S.A.* **2017**, *114*, 4582−4590.

(4) Rhoades, C. C.; Entwistle, D.; Butler, D. The influence of wildfire extent and severity on streamwater chemistry, sediment and temperature following the Hayman Fire, Colorado. *Int. J. Wildland Fire* **2011**, *20*, 430−442.

(5) Bladon, K. D.; Emelko, M. B.; Silins, U.; Stone, M. Wildfire and the future of water supply. *Environ. Sci. Technol.* **2014**, *48*, 8936−8943.

(6) Martin, D. A. At the nexus of fire, water and society. *Philos. Trans. R. Soc., B* **2016**, *371*, 20150172.
(7) Simard, M.; Lecomte, N.; Bergeron, Y.; Bernier, P. Y.; Paré, D. Forest productivity decline caused by successional paludification of boreal soils. *Ecol. Appl.* **2007**, *17*, 1619−1637.
(8) Seely, B.; Welham, C.; Blanco, J. A. Towards the application of soil organic matter as an indicator of forest ecosystem productivity: Deriving thresholds, developing monitoring systems, and evaluating practices. *Ecol. Indicat.* **2010**, *10*, 999−1008.
(9) Woods, S. W.; Birkas, A.; Ahl, R. Spatial variability of soil hydrophobicity after wildfires in Montana and Colorado. *Geomorphology* **2007**, *86*, 465−479.
(10) Lombao, A.; Barreiro, A.; Carballas, T.; Fontúrbel, M. T.; Martín, A.; Vega, J. A.; Fernández, C.; Díaz-Raviña, M. Changes in soil properties after a wildfire in Fragas do Eume Natural Park (Galicia, NW Spain). *Catena* **2015**, *135*, 409−418.
(11) Jiménez-Morillo, N. T.; de la Rosa, J. M.; Waggoner, D.; Almendros, G.; González-Vila, F. J.; González-Pérez, J. A. Fire effects in the molecular structure of soil organic matter fractions under Quercus suber cover. *Catena* **2016**, *145*, 266−273.
(12) González-Pérez, J. A.; González-Vila, F. J.; Almendros, G.; Knicker, H. The effect of fire on soil organic matter - A review. *Environ. Int.* **2004**, *30*, 855−870.
(13) Knicker, H. How does fire affect the nature and stability of soil organic nitrogen and carbon? A review. *Biogeochemistry* **2007**, *85*, 91−118.
(14) Araya, S. N.; Fogel, M. L.; Berhe, A. A. Thermal alteration of soil organic matter properties: A systematic study to infer response of Sierra Nevada climosequence soils to forest fires. *Soil* **2017**, *3*, 31−44.
(15) Alexis, M. A.; Rasse, D. P.; Knicker, H.; Anquetil, C.; Rumpel, C. Evolution of soil organic matter after prescribed fire: A 20-year chronosequence. *Geoderma* **2012**, *189*−*190*, 98−107.
(16) Carlson, D. J.; Reich, P. B.; Frelich, L. E. Fine-scale heterogeneity in overstory composition contributes to heterogeneity of wildfire severity in southern boreal forest. *J. For. Res.* **2011**, *16*, 203−214.
(17) Abney, R. B.; Kuhn, T. J.; Chow, A.; Hockaday, W.; Fogel, M. L.; Berhe, A. A. Pyrogenic carbon erosion after the Rim Fire, Yosemite National Park: The role of burn severity and slope. *J. Geophys. Res.* **2019**, *124*, 432−449.
(18) Ritchie, M. W.; Skinner, C. N.; Hamilton, T. A. Probability of tree survival after wildfire in an interior pine forest of northern California: Effects of thinning and prescribed fire. *For. Ecol. Manag.* **2007**, *247*, 200−208.
(19) Addington, R. N.; Hudson, S. J.; Hiers, J. K.; Hurteau, M. D.; Hutcherson, T. F.; Matusick, G.; Parker, J. M. Relationships among wildfire, prescribed fire, and drought in a fire-prone landscape in the south-eastern United States. *Int. J. Wildland Fire* **2015**, *24*, 778−783.
(20) Pollet, J.; Omi, P. N. Effect of thinning and prescribed burning on crown fire severity in ponderosa pine forests. *Int. J. Wildland Fire* **2002**, *11*, 1−10.
(21) Boer, M. M.; Sadler, R. J.; Wittkuhn, R. S.; McCaw, L.; Grierson, P. F. Long-term impacts of prescribed burning on regional extent and incidence of wildfires − Evidence from 50 years of active fire management in SW Australian forests. *For. Ecol. Manag.* **2009**, *259*, 132−142.
(22) Alcañiz, M.; Outeiro, L.; Francos, M.; Úbeda, X. Effects of prescribed fires on soil properties: A review. *Sci. Total Environ.* **2018**, *613*−*614*, 944−957.
(23) Ranatunga, T. D.; He, Z. Q.; Bhat, K. N.; Zhong, J. Y. Solid-state ^{13}C nuclear magnetic resonance spectroscopic characterization of soil organic matter fractions in a forest ecosystem subjected to prescribed burning and thinning. *Pedosphere* **2017**, *27*, 901−911.
(24) Coates, T. A.; Chow, A. T.; Hagan, D. L.; Wang, G. G.; Bridges, W. C.; Dozier, J. H. Frequent prescribed burning as a long-term practice in longleaf pine forests does not affect detrital chemical composition. *J. Environ. Qual.* **2017**, *46*, 1020−1027.
(25) Faria, S. R.; De la Rosa, J. M.; Knicker, H.; González-Pérez, J. A.; Keizer, J. J. Molecular characterization of wildfire impacts on organic matter in eroded sediments and topsoil in Mediterranean eucalypt stands. *Catena* **2015**, *135*, 29−37.
(26) Miller, A. Z.; De la Rosa, J. M.; Jiménez-Morillo, N. T.; Pereira, M. F. C.; Gonzalez-Perez, J. A.; Knicker, H.; Saiz-Jimenez, C. Impact of wildfires on subsurface volcanic environments: New insights into speleothem chemistry. *Sci. Total Environ.* **2020**, *698*, 134321.
(27) González-Pérez, J. A.; Almendros, G.; de la Rosa, J. M.; González-Vila, F. J. Appraisal of polycyclic aromatic hydrocarbons (PAHs) in environmental matrices by analytical pyrolysis (Py-GC/MS). *J. Anal. Appl. Pyrol.* **2014**, *109*, 1−8.
(28) De la Rosa, J. M.; Faria, S. R.; Varela, M. E.; Knicker, H.; González-Vila, F. J.; González-Pérez, J. A.; Keizer, J. Characterization of wildfire effects on soil organic matter using analytical pyrolysis. *Geoderma* **2012**, *191*, 24−30.
(29) Wang, J. J.; Dahlgren, R. A.; Erşan, M. S.; Karanfil, T.; Chow, A. T. Wildfire altering terrestrial precursors of disinfection byproducts in forest detritus. *Environ. Sci. Technol.* **2015**, *49*, 5921−5929.
(30) Ku, P. J.; Tsui, M. T. K.; Nie, X. P.; Chen, H.; Hoang, T. C.; Blum, J. D.; Dahlgren, R. A.; Chow, A. T. Origin, reactivity, and bioavailability of mercury in wildfire ash. *Environ. Sci. Technol.* **2018**, *52*, 14149−14157.
(31) Wang, J. J.; Dahlgren, R. A.; Chow, A. T. Controlled burning of forest detritus altering spectroscopic characteristics and chlorine reactivity of dissolved organic matter: Effects of temperature and oxygen availability. *Environ. Sci. Technol.* **2015**, *49*, 14019−14027.
(32) Song, J. Z.; Peng, P. A. Characterisation of black carbon materials by pyrolysis-gas chromatography-mass spectrometry. *J. Anal. Appl. Pyrol.* **2010**, *87*, 129−137.
(33) Chen, H.; Blosser, G. D.; Majidzadeh, H.; Liu, X. J.; Conner, W. H.; Chow, A. T. Integration of an automated identification-quantification pipeline and statistical techniques for pyrolysis GC/MS tracking of the molecular fingerprints of natural organic matter. *J. Anal. Appl. Pyrol.* **2018**, *134*, 371−380.
(34) Schellekens, J.; Almeida-Santos, T.; Macedo, R. S.; Buurman, P.; Kuyper, T. W.; Vidal-Torrado, P. Molecular composition of several soil organic matter fractions from anthropogenic black soils (Terra Preta de Indio) in Amazonia - A pyrolysis-GC/MS study. *Geoderma* **2017**, *288*, 154−165.
(35) Wang, J. J.; Bowden, R. D.; Lajtha, K.; Washko, S. E.; Wurzbacher, S. J.; Simpson, M. J. Long-term nitrogen addition suppresses microbial degradation, enhances soil carbon storage, and alters the molecular composition of soil organic matter. *Biogeochemistry* **2019**, *142*, 299−313.
(36) Abney, R. B.; Jin, L.; Berhe, A. A. Soil properties and combustion temperature: Controls on the decomposition rate of pyrogenic organic matter. *Catena* **2019**, *182*, 104127.
(37) Galili, T. dendextend: An R package for visualizing, adjusting and comparing trees of hierarchical clustering. *Bioinformatics* **2015**, *31*, 3718−3720.
(38) Kaal, J.; Cortizas, A. M.; Nierop, K. G. J. Characterisation of aged charcoal using a coil probe pyrolysis-GC/MS method optimised for black carbon. *J. Anal. Appl. Pyrol.* **2009**, *85*, 408−416.
(39) Neff, J. C.; Townsend, A. R.; Gleixner, G.; Lehman, S. J.; Turnbull, J.; Bowman, W. D. Variable effects of nitrogen additions on the stability and turnover of soil carbon. *Nature* **2002**, *419*, 915−917.
(40) Nowakowski, D. J.; Jones, J. M.; Brydson, R. M. D.; Ross, A. B. Potassium catalysis in the pyrolysis behaviour of short rotation willow coppice. *Fuel* **2007**, *86*, 2389−2402.
(41) Kaal, J.; Wagner, S.; Jaffé, R. Molecular properties of ultrafiltered dissolved organic matter and dissolved black carbon in headwater streams as determined by pyrolysis-GC-MS. *J. Anal. Appl. Pyrol.* **2016**, *118*, 181−191.
(42) Kaal, J.; Schneider, M. P. W.; Schmidt, M. W. I. Rapid molecular screening of black carbon (biochar) thermosequences obtained from chestnut wood and rice straw: A pyrolysis-GC/MS study. *Biomass Bioenergy* **2012**, *45*, 115−129.
(43) Bodí, M. B.; Martin, D. A.; Balfour, V. N.; Santín, C.; Doerr, S. H.; Pereira, P.; Cerdà, A.; Mataix-Solera, J. Wildland fire ash:

https://doi.org/10.1021/acs.est.2c00426
Environ. Sci. Technol. XXXX, XXX, XXX−XXX

Production, composition and eco-hydro-geomorphic effects. *Earth-Sci. Rev.* **2014**, *130*, 103−127.
(44) Bonanomi, G.; Incerti, G.; Barile, E.; Capodilupo, M.; Antignani, V.; Mingo, A.; Lanzotti, V.; Scala, F.; Mazzoleni, S. Phytotoxicity, not nitrogen immobilization, explains plant litter inhibitory effects: Evidence from solid-state ^{13}C NMR spectroscopy. *New Phytol.* **2011**, *191*, 1018−1030.
(45) Knicker, H.; Almendros, G.; González-Vila, F. J.; González-Pérez, J. A.; Polvillo, O. Characteristic alterations of quantity and quality of soil organic matter caused by forest fires in continental Mediterranean ecosystems: A solid-state ^{13}C NMR study. *Eur. J. Soil Sci.* **2006**, *57*, 558−569.
(46) Kaal, J.; Martínez Cortizas, A. M.; Reyes, O.; Soliño, M. Molecular characterization of *Ulex europaeus* biochar obtained from laboratory heat treatment experiments - A pyrolysis-GC/MS study. *J. Anal. Appl. Pyrol.* **2012**, *95*, 205−212.
(47) Mullen, C. A.; Boateng, A. A. Catalytic pyrolysis-GC/MS of lignin from several sources. *Fuel Process. Technol.* **2010**, *91*, 1446−1458.
(48) Shen, D. K.; Gu, S.; Luo, K. H.; Wang, S. R.; Fang, M. X. The pyrolytic degradation of wood-derived lignin from pulping process. *Bioresour. Technol.* **2010**, *101*, 6136−6146.
(49) Kaal, J.; Brodowski, S.; Baldock, J. A.; Nierop, K. G. J.; Cortizas, A. M. Characterisation of aged black carbon using pyrolysis-GC/MS, thermally assisted hydrolysis and methylation (THM), direct and cross-polarisation ^{13}C nuclear magnetic resonance (DP/CP NMR) and the benzenepolycarboxylic acid (BPCA) method. *Org. Geochem.* **2008**, *39*, 1415−1426.
(50) Kaal, J.; Rumpel, C. Can pyrolysis-GC/MS be used to estimate the degree of thermal alteration of black carbon? *Org. Geochem.* **2009**, *40*, 1179−1187.
(51) Alexis, M. A.; Rumpel, C.; Knicker, H.; Leifeld, J.; Rasse, D.; Péchot, N.; Bardoux, G.; Mariotti, A. Thermal alteration of organic matter during a shrubland fire: A field study. *Org. Geochem.* **2010**, *41*, 690−697.
(52) Buurman, P.; Peterse, F.; Almendros Martin, G. A. Soil organic matter chemistry in allophanic soils: A pyrolysis-GC/MS study of a Costa Rican Andosol catena. *Eur. J. Soil Sci.* **2007**, *58*, 1330−1347.
(53) Scharenbroch, B. C.; Nix, B.; Jacobs, K. A.; Bowles, M. L. Two decades of low-severity prescribed fire increases soil nutrient availability in a Midwestern, USA oak (*Quercus*) forest. *Geoderma* **2012**, *183*−*184*, 80−91.
(54) Kaal, J.; Martínez Cortizas, A. M.; Eckmeier, E.; Costa Casais, M. C.; Santos Estévez, M. S.; Criado Boado, F. C. Holocene fire history of black colluvial soils revealed by pyrolysis-GC/MS: A case study from Campo Lameiro (NW Spain). *J. Archaeol. Sci.* **2008**, *35*, 2133−2143.
(55) Weiss, N.; Kaal, J. Characterization of labile organic matter in Pleistocene permafrost (NE Siberia), using thermally assisted hydrolysis and methylation (THM-GC-MS). *Soil Biol. Biochem.* **2018**, *117*, 203−213.
(56) Parnaudeau, V.; Dignac, M. F. The organic matter composition of various wastewater sludges and their neutral detergent fractions as revealed by pyrolysis-GC/MS. *J. Anal. Appl. Pyrol.* **2007**, *78*, 140−152.
(57) Lv, G. J.; Wu, S. B. Analytical pyrolysis studies of corn stalk and its three main components by TG-MS and Py-GC/MS. *J. Anal. Appl. Pyrol.* **2012**, *97*, 11−18.
(58) Budai, A.; Calucci, L.; Rasse, D. P.; Strand, L. T.; Pengerud, A.; Wiedemeier, D.; Abiven, S.; Forte, C. Effects of pyrolysis conditions on *Miscanthus* and corncob chars: Characterization by IR, solid state NMR and BPCA analysis. *J. Anal. Appl. Pyrol.* **2017**, *128*, 335−345.
(59) Xu, Z. X.; Xu, L.; Cheng, J. H.; He, Z. X.; Wang, Q.; Hu, X. Investigation of pathways for transformation of N-heterocycle compounds during sewage sludge pyrolysis process. *Fuel Process. Technol.* **2018**, *182*, 37−44.
(60) Kaal, J.; Martínez-Cortizas, A.; Nierop, K. G. J.; Buurman, P. A detailed pyrolysis-GC/MS analysis of a black carbon-rich acidic colluvial soil (Atlantic ranker) from NW Spain. *Appl. Geochem.* **2008**, *23*, 2395−2405.

https://doi.org/10.1021/acs.est.2c00426
Environ. Sci. Technol. XXXX, XXX, XXX−XXX